PHOTOCONDUCTIVITY AND PHOTOLUMINESCENCE SPECTRA OF $CdIn_2S_4$:Ti CRYSTALS

O. Kulikova, L. Kulyuk, A. Siminel, and V. Tezlevan

Institute of Applied Physics, Academy of Sciences of Moldova, 5, Academiei str., MD-2028, Chisinau, Republic of Moldova

(Received 23 June 2009)

1. Introduction

Spinel type crystals doped with transition metal ions attract considerable attention due to their possible laser applications [1].

$CdIn_2S_4$ crystals doped with Cr ions (ionic radius 0.62 Å) in a charge state Cr^{+3} were studied earlier [2-4]. Crystals doped with other transition metals, for example, Ti, are also promising for laser applications [5-8]. In this paper optical properties of titanium ions (Ti^{+3} ionic radius amounts to 0.67 Å) in a $CdIn_2S_4$ semiconductor crystalline matrix were studied.

We present the results of an experimental study of the steady-state photoluminescence (PL) and photoconductivity (PC) spectra of $CdIn_{2(1-x)}Ti_{2x}S_4$ spinel type single crystals with Ti concentration ($0.001 \leq x \leq 0.05$).

2. Samples and experiment

Bulk stoichiometric $CdIn_2S_4$:Ti crystals with the Ti impurity concentration of 0.02-0.9 at % were grown by a closed tube vapor method with iodine as a transport agent.

The crystals with a low impurity concentration are light red; with increasing of the Ti concentration to more than 0.2 at % they become dark brown. The spectral position of PL excitation was chosen taking into account the spectral positions of the observed PC peaks E_{PC1} (the second harmonic of YAG:Nd laser, λ_{ex1}=532nm) and E_{PC2} (He-Ne laser, λ_{ex2}=633 nm). The steady-state photoluminescence measurements were carried out in the range of 500-2000 nm in a temperature interval of 80-300 K. The emission spectra were detected using a PbS cell or photomultiplier.

3. Results

3.1. PC spectra

The PC spectra of $CdIn_2S_4$:Ti at 300 and 80 K are presented in Fig. 1. The curve of the photoconductivity spectrum at 80 K (curve 2) consists of two peaks with maxima at $\hbar\omega \sim$ 2.5 eV and $\hbar\omega \sim$ 2.3 eV.

The position of the edge peak at $\hbar\omega \sim$ 2.5 eV corresponds to the characteristic region of optical absorption spectra and corresponds to the interband transitions in undoped samples [9].

The E_g^{ind} value estimated from PC spectra according to the dependence of σ vs $h\nu$ amounts to 2.3 eV (300 K) and 2.5 eV (80 K) The values of E_g are higher than those determined from the absorption spectra earlier [10].

The PC spectral peak at E_{PC2}=2.05 eV (T = 300 K) can be assigned to the electron transitions from an acceptor level to the conduction band. [9]. The PC spectral peak at E_{PC1}=2.3eV (80 K) is attributed to the presence of Ti ions in the host crystal.

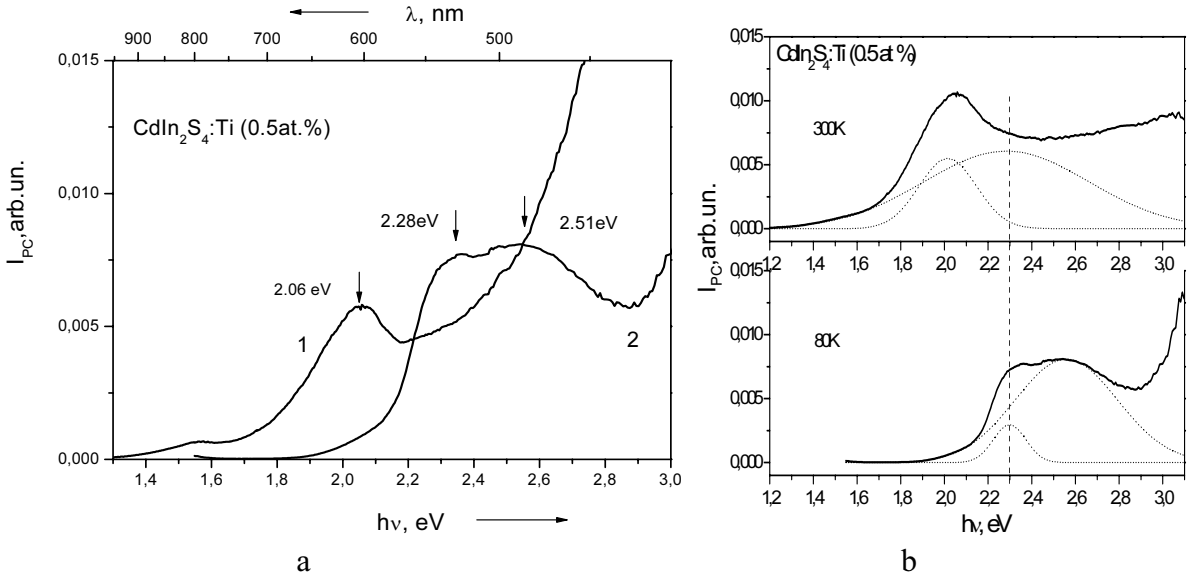

Fig. 1. Photoconductivity spectra of $CdIn_2S_4$:Ti (0. 5 at %) crystals at 300 (1) and 80 K (2).

The energy position of the peaks of photoconductivity corresponds to the green and red spectral range; this determined the choice of the energy of laser excitation when we studied the photoluminescence spectra.

3.2. PL spectra

The concentration dependence of the PL spectra of Ti impurities in $CdIn_2S_4$:Ti at the excitation (λ_{ex1} =532 nm) is shown in Fig. 2. The contribution of the impurity band at low concentrations exhibits a long wavelength shoulder. With the increasing of the impurity concentration the emission band of Ti ions becomes more pronounced.

The PL spectral maximum of the samples with a small Ti concentration (less than 0.05 at %) is located at 1.65 eV and corresponds to the radiative recombination of the excited carriers via intrinsic defects of the undoped $CdIn_2S_4$ [10]. The nature of these defects is associated with the inverted spinel-like structure [11].

When the Ti concentration exceeds 0.05%, the intrinsic $CdIn_2S_4$ luminescense is quenched owing to the intra-center titanium radiation. The relatively heavily doped samples (0.2 at %) exhibit an infrared broad band emission centered at 1.32 eV.

Under the green excitation (E_{ex1}), the steady-state PL spectra of $CdIn_2S_4$:Ti crystals consist of two broad bands centered at E_{PL1}=1.32 eV and E_{PL2}=1.65 eV. (Fig. 3). The input of the recombination radiation stipulated by the defect matrix states increases at the short wavelength excitation λ_{ex1} = 532 nm ($\hbar\omega_{ex}$=2.33 eV $\approx E_g^{ind}$) as well as with the temperature decreasing (Fig. 3).

At room temperature, the shape of the integral spectrum is virtually determined by the second broad band E_{PL2}. At the red excitation (E_{ex2}) this component provides the main contribution to the PL spectra in the whole temperature range.

As it is shown in Fig. 2, the increasing of the impurity concentration leads to the quenching of the luminescence, that can be explained by the formation of efficient centers of nonradiative recombination. At the Ti concentration of ~0.9 at %, the luminescence owing to the Ti impurities is completely quenched.

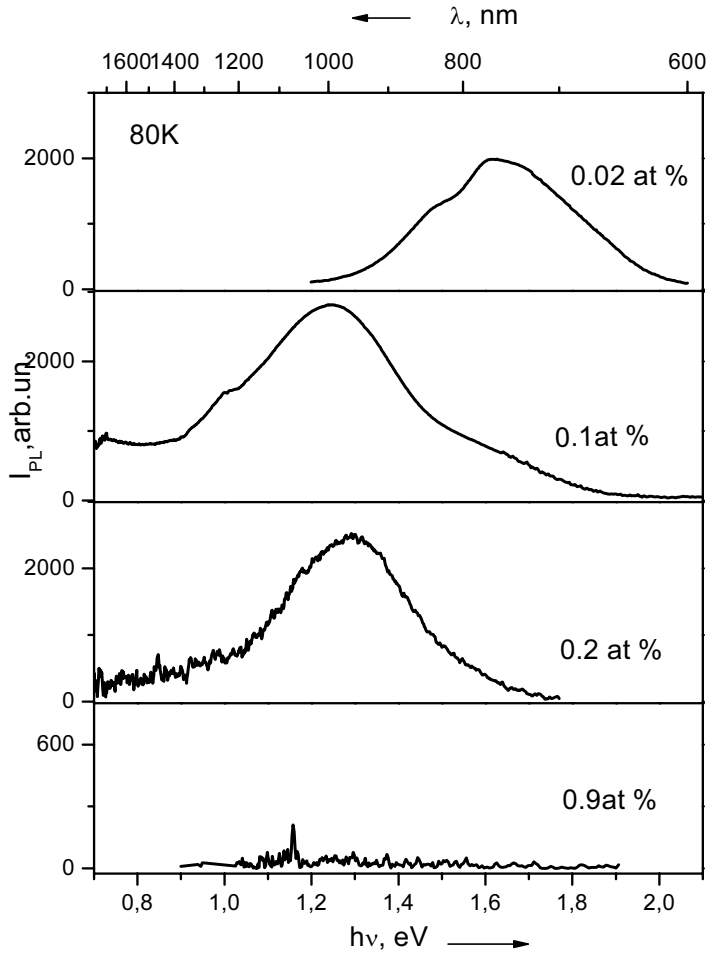

Fig. 2. PL spectra of $CdIn_2S_4$:Ti ($0.02 \leq x \leq 0.9$ at %) at T = 80 K.

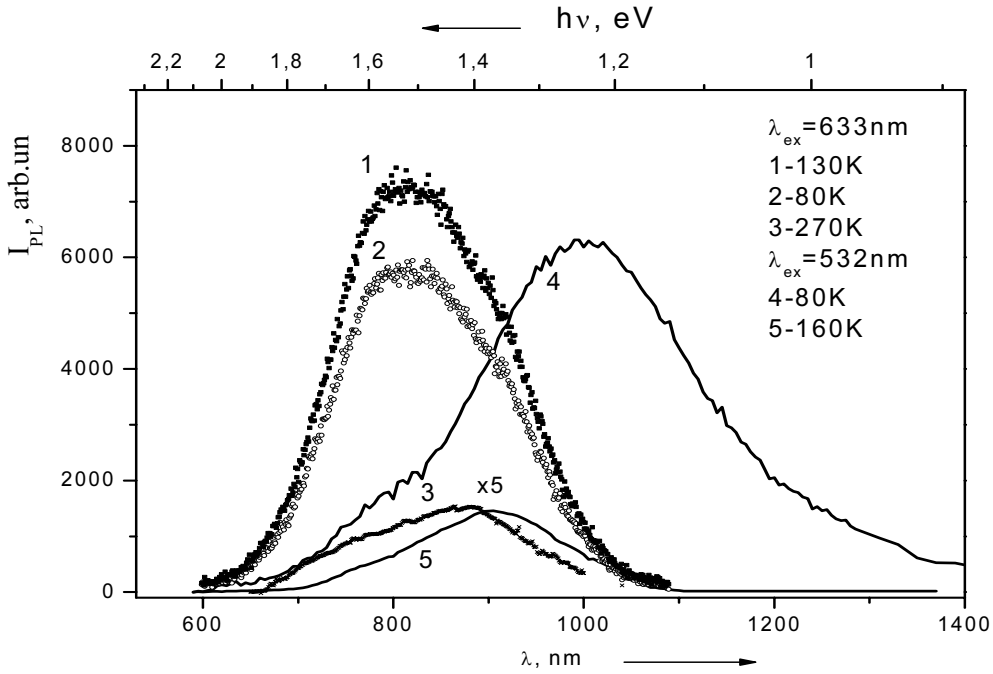

Fig. 3. Photoluminescence spectra of $CdIn_2S_4$:Ti crystals (0.05 at % Ti) at various temperature at red (λ_{ex2} =633 nm; curves *1-3*) and green (λ_{ex1} =532 nm; curves *4-5*) excitation.

4. Discussion

The authors of paper [9] studied the photoconductivity spectra of undoped $CdIn_2S_4$ and proposed a band diagram with a deep acceptor level 0.25 eV above the valence band top. The study of the PC spectrum in $CdIn_2S_4$:Ti (Fig. 1b) has shown that the PC curves can be represented as a resulting spectrum of two Gaussian functions. The spectral band at 2.3 eV corresponds to the titanium PC spectrum; the deep Ti level (the main state of titanium ions) is located below the acceptor level associated with In_{Cd} defects; that is, it is located near the valence band, and this can elucidate some peculiarities in the PL spectrum.

As in the case of α-$ZnAl_2S_4$:Ti spinel type crystals [12], the Ti impurities in $CdIn_2S_4$ do not exhibit an EPR signal, since Ti^{3+} valence states are absent.

The increasing of the impurity concentration leads to the quenching of luminescence; this can be explained by the formation of efficient centers of nonradiative recombination.

This suggests that there are no Ti^{3+} valence states in this case. Since $CdIn_2S_4$ is a wide band gap semiconductor, we assign the observed IR emission bands to the ligand to Ti^{4+} charge transfer transitions. The observed PL spectra in terms of the cluster composed of the central Ti^{4+} ion and six sulfur atoms, i.e., $Ti^{4+}S_6^{2-}$ complex. The ground state of this cluster is the $^1A_{1g}$ state.

On the basis of the assumption of a charge transfer transition from sulfur to Ti^{4+} ions in the $Ti^{4+}S_6^{2-}$ complex, the observed broad bands in PL and PC spectra were interpreted using the models proposed in [1, 5].

The following mechanism was proposed:

1) the Ti^{4+} ion is octahedrically coordinated with six S^{2-} ions,
2) the charge transfer excitation is induced from S^{2-} into an empty 3d orbital, resulting in Ti^{3+} in the electronic excited state,
3) the excited 3d electron interacts with the lattice vibrations; its return to the ground state results in the Stokes shift, and finally this excited electron radiatively annihilates emitting photons in the energy range near 1.3 eV.

The position and shapes of PL spectra bands induced by the both excitation lines λ_{ex1} and λ_{ex2} are the same. Taking into account this fact and the positions and shapes of the PL and PC spectral bands at liquid nitrogen temperature, we suggested a single coordinate configuration diagram shown in Fig. 4 that describes optical processes in $CdIn_2S_4$:Ti crystals. At the configuration diagram the allowed transitions $^1T_{1u} \rightarrow {}^1A_{1g}$ are presented. The PL transition $^3T_{1u} \rightarrow {}^1A_{1g}$ is spin forbidden, though the dipole one is allowed. On the basis of these considerations, we assume that the two observed IR bands can be probably assigned to transitions $^3T_{1u} \rightarrow {}^1A_{1g}$ and $^1T_{1u} \rightarrow {}^1A_{1g}$.

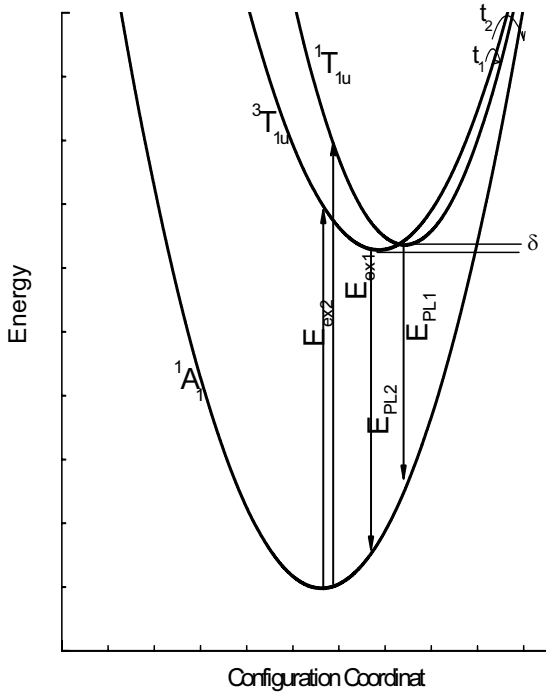

Fig. 4. Schematic diagram of the adiabatic potential.

E_{ex} are the processes associated with the population of Ti^{+3} ions dependent on the excitation energy; E_{PL} are radiative transitions to the $^2T_2$ level; t_1 are thermally activated nonradiative transitions; t_2 are nonradiative tunnel transitions dependent on the concentration of Ti^{+3} ions.

The energy spectrum of the complex can be schematically illustrated by four adiabatic potential sheets. The ground adiabatic potential sheet looks as follows

$$U_{^1A1} = \frac{\hbar\omega}{2} q^2, \tag{1}$$

where $\hbar\omega$ is the energy of the vibrational quantum. The expression for the first excited sheet

$$U_{^3T_1} = \frac{\hbar\omega}{2} q^2 + \Delta_1 + \upsilon_1 q \tag{2}$$

includes the energy gap Δ_1 between the $^1A_1$ and $^3T_1$ states in the rigid lattice as well as the term responsible for the interaction of the $^3T_1$ state of TiS_6 complex with the full symmetric vibration of this complex, where υ_1 is the vibronic constant. Analogously, the second excited sheet can be described by the expression

$$U_{^1T_1} = \frac{\hbar\omega}{2} q^2 + \Delta_2 + \upsilon_2 q\,, \tag{3}$$

where Δ_2 denotes the energy gap between the states $^1A_1$ and $^1T_1$, and υ_2 is the vibronic parameter characterizing the interaction of the $^1T_1$ state with the breathing mode of the complex.

First, comparing the absorption spectra and the low temperature luminescence spectra under the green excitation we ascribe the photoconductivity band at ≈2.3 eV to the transition $^1A_1 \rightarrow {}^1T_1$.

This immediately gives the value 18552 cm^{-1} for the energy gap Δ_2. Assuming that under the excitation by the red light ($\lambda = 633\,nm$, 1.9 eV) one gets straight into the adiabatic potential $U_{^3T_1}$, we obtain Δ_1=15325 cm^{-1}. At the next stage we use the experimental data on the luminescence spectra and determine with the aid of these data the vibronic coupling constants υ_1 and υ_2.

Actually the maxima of the luminescence bands under the red ($\hbar\omega_{PL1}$) and the green ($\hbar\omega_{PL2}$) excitation can be described in the adiabatic approximation by the relations

$$\hbar\omega_{pL_1} = \Delta_1 - \upsilon_1^2/\hbar\omega;\;\; \hbar\omega_{pL_2} = \Delta_2 - \upsilon_2^2/\hbar\omega\,. \tag{4}$$

For $\hbar\omega_{PL1}$ = 1.6 eV = 12902 cm^{-1}, $\hbar\omega_{PL2}$ =1.3 eV = 10486 cm^{-1}, Δ_1=15325 cm^{-1} and Δ_2=18552 cm^{-1} we obtain from Eq. (5) the following values of the vibronic coupling constants $\upsilon_1 = 941\,cm^{-1}$, and $\upsilon_2 = 1718\,cm^{-1}$.

Then, using these values of the vibronic constants and $\omega = 366\,cm^{-1}$ we calculate the height of the activation barrier (Fig. 4)

$$\delta = \frac{\hbar\omega}{2}\left(\frac{\Delta_1 - \Delta_2}{\upsilon_2 - \upsilon_1} + \frac{\upsilon_2}{\hbar\omega}\right)^2 \approx 66\,cm^{-1} = 90\,K = 0.008eV\,. \tag{5}$$

From Eq. (4) it follows that the $^1T_{1u}$ level is not populated under the red excitation (Fig. 3).

The thermally activated nonradiative transitions t_1 are responsible for the position and the shape of the radiation curves at various excitation levels and temperature. The increasing of the impurity concentration increases the probability of the nonradiative tunnel transitions t_2, this elucidates the decreasing of the PL intensity at 0.05 at % of Ti and its subsequent quenching.

Conclusions

The photoluminescence, photoconductivity, and absorption properties of $CdIn_2S_4$:Ti crystals were studied. Using the obtained data we have suggested a mechanism of optical transitions and a configuration diagram of the adiabatic potentials that elucidates the concentration and temperature dependences of the radiation spectra of the studied crystals.

References

[1] A. Jouini, A. Yoshikawa, A. Brenier, T. Fukuda, and G. Boulon, Phys. Stat. Sol. (c), 4, 1380, (2007).
[2] N. Graber, F. Orfino, and C.F. Schwerdtfeger, Solid St. Comm., 36, 407, (1980).
[3] O. Kulikova, L.L. Kulyuk, S.M. Popov, S.I. Radautsan, and V.E. Tezlevan, J. Crystal Research and Technology, 31, 741, (1996).
[4] O. Kulikova, L.L. Kulyuk, S.M. Popov, V.E. Tezlevan, E. Fortin, Jap. J. of Appl. Phys., 32, 32-33, 484, (1993).
[5] P. Moulton, J. Opt. News, 8, 6, 9, (1982).
[6] W.C. Wong, D.S. McClure, S.A. Basun, and M.R. Kokta, Phys. Rev. B, 51, 5682, (1995).
[7] L.E. Bausă, I. Vergar, and J. Garcfa-Solė, W. J. Appl. Phys., 68, 2, 736, (1990).
[8] M. Yamaga, B. Henderson, K.P.O. Donnell, F. Rasheed, Y. Gao, and B. Cockayne, Appl. Phys. B, 52, 225, (1991).
[9] A. Aneda, L. Garbato, F. Raga, and A. Serpi, Phys. Stat. Sol. (a), 50, 643, (1978); S. Charbonneau, E. Fortin, and A. Aneda, Phys. Rev. B, 31, 2326, (1985).
[10] O.V. Kulikova, L.L. Kulyuk, S.I. Radautsan, S.A. Ratseev, E.E. Strumban, V.E. Tezlevan, and V.I. Tsitsanu, Phys. Stat. Sol. (a), 107, 373, (1988).
[11] W. Czaja, Helv. Phys. Acta, 40, 352, (1967).
[12] L. Kulyuk, E. Fortin, K. Sushkevich, T. Dumochel, and D. Koshchug, Book of Abstracts ICTMC-15 Conference, March 6-10, Kyoto, JAPAN, Thu-O-8B, (2006).